

Figure 7, indicates that increase or decrease in chlorophyll is in accordance with previous week's wind pattern, i.e. with a time lag of one week. It can be seen from Figure 7 that wind speed is less in 2003 in the fourth week of January compared to the same in 2004 and 2005. This gets reflected in chlorophyll pattern of the first week of February, in the form of lower chlorophyll in 2003. For the remaining period, chlorophyll content in 2003 is higher compared to that in 2004 and 2005. Accordingly, wind speed of the previous week is always more in 2003.

Inter-annual variance in chlorophyll of deep waters of the NAS is observed from satellite and ship data. Though northeasterly winds over the Arabian Sea are seasonally regular, there are variations in their magnitude from year to year. Variations in chlorophyll pattern in these waters are consistent with those in the prevailing northeasterly winds. This happens through a combined mechanism of wind-induced increase in density and Ekman depth, which causes nutrient enrichment in euphotic depth. Thus, the two parameters, biological (chlorophyll) and physical (wind, surface density, etc.) co-vary and the response of chlorophyll to changing wind pattern is observed with time lag of one to two weeks. For this reason, wind can be used as an indicator to predict chlorophyll pattern.

1. Banse, K. and McClain, C. R., *Mar. Ecol. Prog. Ser.*, 1986, 201–211.
2. Barber, R. T. and Chavez, F. P., *Limnol. Oceanogr.*, 1991, **36**, 1803–1815.
3. Madhupratap, M., Prasannakumar, S., Bhattathiri, P. M. A., Dileepkumar, M., Raghukumar, S., Nair, K. K. C. and Ramaiah, N., *Nature*, 1996, **384**, 549–552.
4. Prasanna Kumar, S., Madhupratap, M., Dileep Kumar, M., Gauns, M., Muraleedharan, P. M., Sarma, V. V. S. and De Souza, S. N., *Deep Sea Res.*, 2000, 433–441.
5. Matondkar, S. G. P., Bhatt, S. R., Dwivedi, R. M. and Nayak, S. R., *Harmful Algae News, IOC Newsl.*, pp. 4–5.
6. Gordon, H. R., *J. Geophys. Res.*, 1997, **102**, 17081–17106.
7. Gordon, H. R. and Wang, M., *Appl. Opt.*, 1994, **33**, 443–452.
8. O'Reilly, J. E., Maritonena Mitchell, B. G., Siegal, D. A., Carder, K. L., Graver, S. A., Kahru, M. and McClain, C. R., *J. Geophys. Res.*, 1998, **103**, 24937–24963.
9. Chauhan, P., Mohan, M. and Nayak, S., *Proceedings 4th Berlin Workshop on Remote Sensing '5 Years of MOS-IRS*, 2001, pp. 45–61.

ACKNOWLEDGEMENTS. We are grateful to the Centre for Marine Living Resources, Department of Ocean Development, Govt of India for extending services of research vessel, FORV *Sagar Sampada*, to carry out *in situ* observations during winter bloom in the northern Arabian Sea for two consecutive years.

Received 21 February 2005; revised accepted 31 January 2006

Crustal structure at the epicentral zone of the 2005 Kashmir (Muzaffarabad) earthquake and seismotectonic significance of lithospheric flexure

D. C. Mishra* and R. P. Rajasekhar

National Geophysical Research Institute, Hyderabad 500 007, India

The Bouguer anomaly map of the epicentral zone of Kashmir earthquake is compiled from different sources. The observed gravity high related to Lahore–Sargodha ridge is attributed to flexural bulge due to collision of the Indian and Eurasian plates. A gravity profile is modelled across this region constrained from the available deep seismic sounding profiles, which suggest a flexural bulge of 3–4 km due to the load of the Himalayas. The hypocentre of this earthquake at a depth of 26 km lies at the junction of this flexural bulge with crustal thickening (70–72 km) towards the north under the Karakoram–Hindukush ranges, which represent the central core complex of collision tectonics. In fact, the hypocentres of all major seismic activities along the Southern Himalayan Front, which are mostly confined between 5–10 and 30–35 km coincide with this junction. These levels may represent shallow decollement plane and an intermediate weak zone caused by differential stress due to plate movement and flexural bulge, that would have caused extension and compression in the upper and lower crusts respectively. The depth to intermediate crustal zone under the Himalayas and Tibet approximately coincides with the effective elastic thickness in this region, implying weak part of the crust that may be caused by the presence of fluids.

Keywords: Effective elastic thickness, flexural bulge, gravity anomalies, Himalayan seismicity, Muzaffarabad earthquake.

THE Himalayan collision zone is one of the most active plate boundaries that generated several large and great earthquakes¹. The recent Kashmir earthquake² of magnitude of 7.6 with focal depth of about 26 km occurred south of the Main Boundary Thrust (MBT), where it takes an inverted U-turn from NNW to SSE (Figure 1). Historically, this region known as Hazara Kashmir Seismic Zone (HKSZ) along with the Hindukush Seismic Zone (HSZ), NW of it, forms an active zone³ (Figure 1). The inverted U-turn of MBT and other tectonic elements of this region forms the Hazara Kashmir Syntaxis. Two major trends, viz. N–S of the Sullaiman range and E–W of the Himalayan range interact in this section to form the syntaxis. Such turns and interactions of trends form the knot, which is the most preferred site for stress accumulation.

*For correspondence. (e-mail: dcm_ngri@yahoo.co.in)

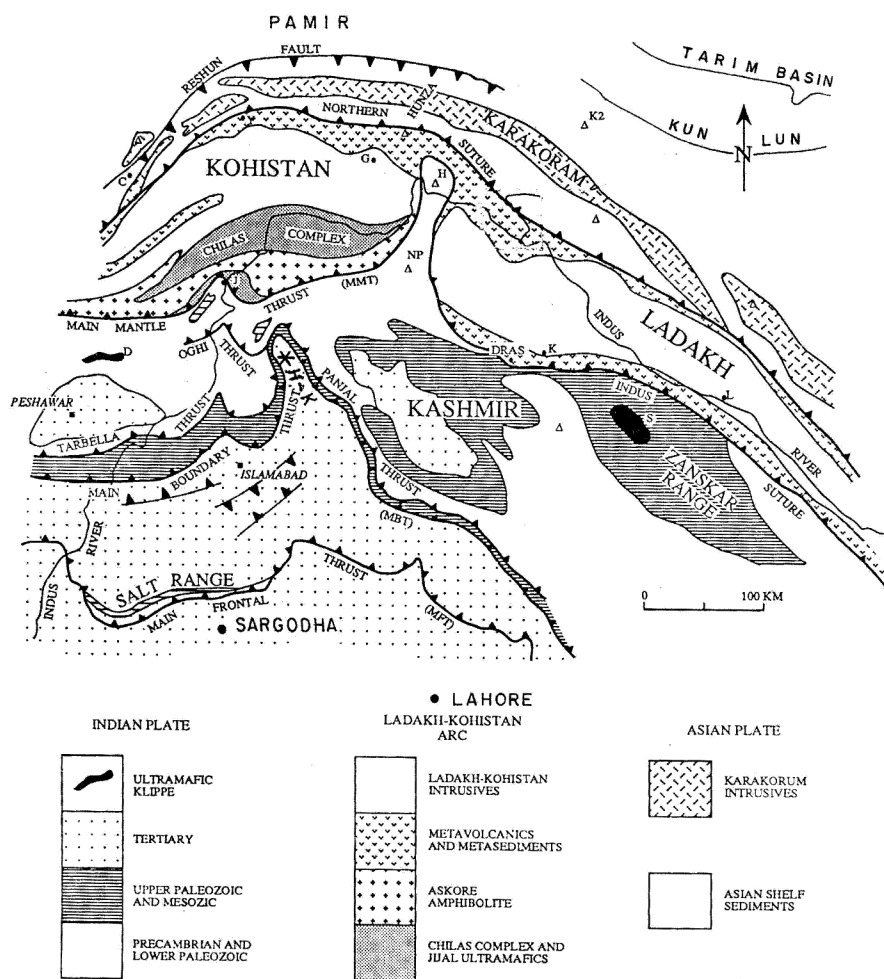


Figure 1. Generalized tectonic map of northwest Himalaya³⁴ with epicentre of present earthquake shown by star². C, Chitral; D, Dargi Klippe; H, Haramosh; G, Gilsit; J, Jijal; K, Kargil; L, Leh; NP, Nanga Parbat; S, Spongtag Klippe; Y, Yasin; H-K, Hazara Kashmir Syntaxis.

This region is also characterized by the presence of several thrusts of local and regional importance in this region (Figure 1).

The earlier Bouguer anomaly map of a section of this region⁴ has been updated by Caproli⁵, which provides significant details of the tectonics of this region. Another Bouguer anomaly map of the whole region⁶ is available on a regional scale. The two maps are digitized and a part from the latter (SW part, Figure 2) is merged with the former to provide the Bouguer anomaly map of a larger block, including the epicentral zone of the present earthquake (Figure 2). This map shows a gravity high (H1) due to Lahore–Sargodha ridge, which is attributed to flexural bulge due to the load of the Himalayas caused by collision of the Indian and Eurasian plates and related subduction. North of this gravity high are the gravity lows (L1 and L2) and large gravity gradients between them signifying MBT and Main Mantle Thrust (MMT; Figure 1). Further north of it are gravity gradients due to the Kunlun and

Altyn Tugh Faults (ATF) and a small gravity high (H2) associated with the latter. The gravity high H3 and low L3 coincide with Tarim Basin and Pamir ranges respectively, representing high and low density intrusives. Gravity lows L1 and L2 forming the Karakoram–Hindukush ranges define the western Himalayan syntaxis. This map also shows the epicentre of the present earthquake, where gravity anomaly shows specific nosing of contours related to inverted U-turn of MBT and Kohistan Arc north of it (Figure 1).

Figure 3 shows northern part of the geoid-corrected low-pass-filtered Bouguer anomaly map of India, with linear gravity highs (H1–H3) in the Himalayan Foredeep related to the flexural bulge, which extends NW to coincide with the Lahore–Sargodha ridge⁷. Figure 3 also shows the distribution of major earthquakes along Southern Himalayan Front since 1670 (ref. 2), which mainly coincide with the gradient of the gravity highs (H1–H3) due to lithospheric flexure and gravity low towards the north

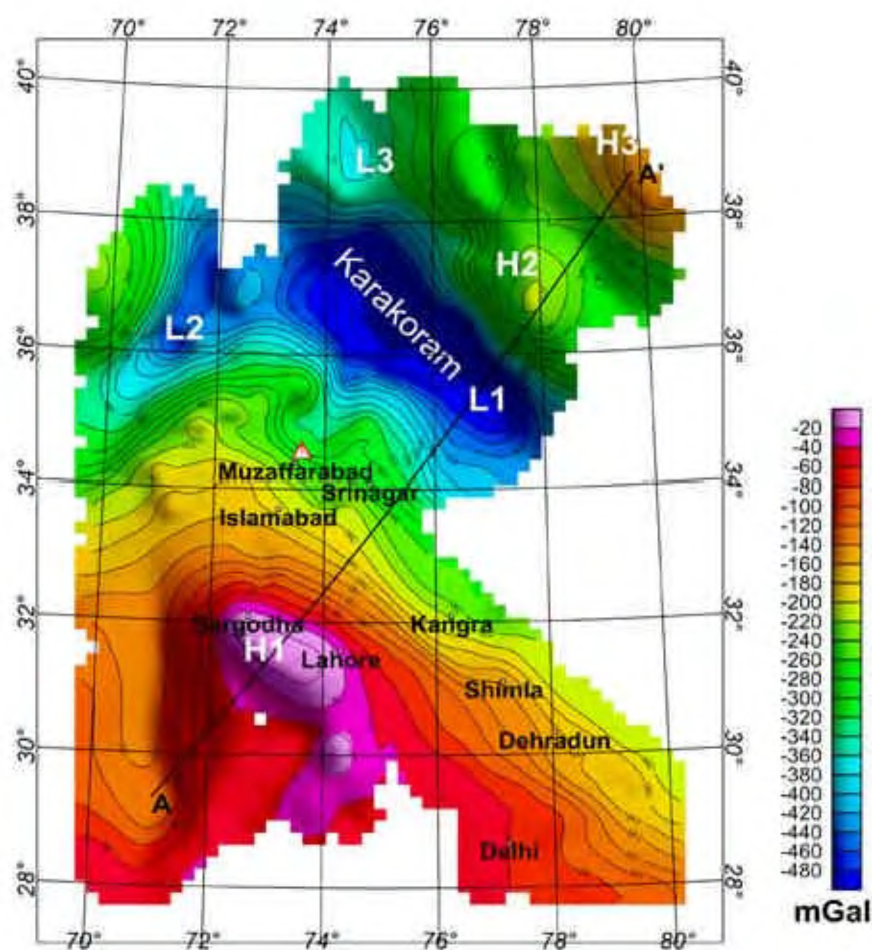


Figure 2. Bouguer anomaly map of a part of NW Himalaya^{5,6}. Triangle shows epicentre of the present earthquake, which lies over the gradient between gravity high H1 and low L1. H1 corresponds to Lahore–Sargodha ridge caused by lithospheric flexure and gravity lows L1 and L2 over the Karakoram–Hindukush ranges are primarily related to crustal thickening and define the western syntaxial axis.

due to crustal thickening. It may be mentioned here that due to non-availability of gravity data over the Himalayas and Tibet, the map for this region is missing in Figure 3, but gravity low towards the north acquires a low value of about -550 mGal along a profile over the central part of Tibet, where the crust thickens⁸ to about 70 – 72 km. Some of the important large and great earthquakes reported along this front are Kangra (1905), Bihar–Nepal (1934), Assam (1950) and Shillong (1897) earthquakes² and some recent examples are Chamoli (1999) and Uttarkashi (1991) earthquakes, which are plotted on Figure 3. It is true even in the case of the HKSZ and HSZ (Figure 3), where epicentres of present and deep focus earthquakes respectively, are located and on extrapolation, they can be visualized to coincide with the gradient of gravity high due to flexural bulge towards the south and gravity low due to crustal thickening towards the north (Figure 2).

Mishra¹⁰ modelled gravity profiles extending from south of Srinagar to Alai mountains across the Great Himalayas (Nanga Parbat), Kohistan Arc and Pamir ranges con-

strained in parts from seismic sections^{11,12}. He suggested that the crustal thickness in this region changes from about 58 – 72 km (maximum) under the Karakoram and Pamir ranges. The crustal model also provided low-density intrusives under the Pamir ranges and a low density layer in the lower crust at a depth of 35 – 37 km under the Karakoram ranges, related with low velocity layer in seismic investigations¹¹. Duroy *et al.*¹³ modelled a gravity profile extending from south of Sargodha high to Pamir ranges constrained from a seismic profile in the middle and suggested mid-crustal high-density rocks for Sargodha High and crustal thickening up to 65 km under Pamir ranges. Based on gravity modelling, Malinconico Jr.¹⁴ has shown the presence of low-density crustal rocks below the Moho in the mantle and high density mantle material subducted in the asthenosphere along the Main Karakoram Thrust, indicating the effect of subduction in this region.

A two-dimensional spectrum of the Bouguer anomaly map (Figure 2) provides approximate depth to subsurface density inhomogeneity through spectral decay rate¹⁵,

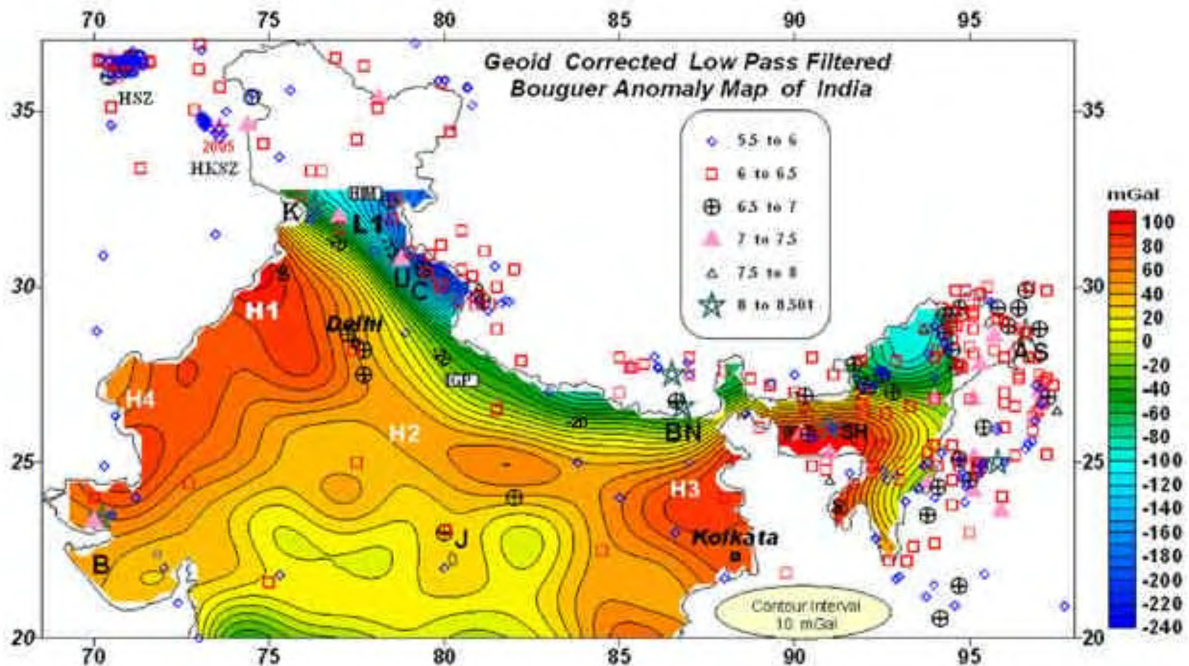


Figure 3. A low-pass-filtered Bouguer anomaly map of India⁷ showing gravity high H1–H3 related to lithospheric flexure in Himalayan Foredeep (IGP = Indo-Gangatic Plains). Epicentres of major earthquakes along Southern Himalayan Front² are shown by different symbols with respect to magnitude. HSZ, Hindukush Seismic Zone and HKSZ, Harzara Kashmir Seismic Zone, which also coincide with the gradient between gravity highs (H1–H3) due to lithospheric flexure and gravity low (L1) due to crustal thickening extrapolated towards the north, as shown in Figure 2. The lowest gravity value of -550 mGal is reported over Tibet⁸. Some large and great earthquakes shown by symbols are: K, Kangra (1905); U, Uttarkashi (1991); C, Chamoli (1999); BN, Bihar–Nepal (1934); SH, Shillong (1897); AS, Assam (1950); B, Bhuj (2001) and J, Jabalpur (1997) earthquakes.

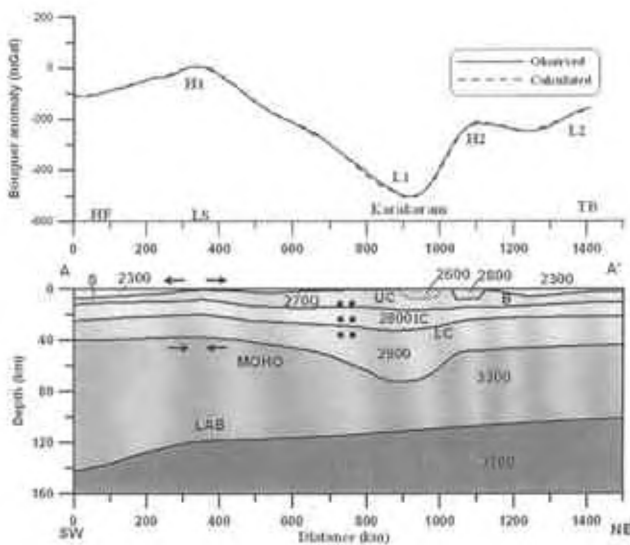


Figure 4. Modelled crustal section along profile AA' (Figure 2). It shows five interfaces related to Lithosphere–Asthenosphere Boundary (LAB), Moho, Lower (LC), Intermediate (IC) and Upper (UC) Crusts, the basement (B) and the sediments (S). Density is given in each layer in kg/m^3 . Some high and low density bodies are shown at the surface to explain small wavelength anomalies which may represent basic and felsic intrusives, respectively. HF, Himalayan Foredeep; LS, Lahore–Sargodha ridge and TB, Tarim basin. Arrows indicate direction of forces due to lithospheric flexure, which represent extension in the upper crust and compression in the lower crust causing differential stress in the crust. Small dots in the model at 10 km and in the depth range of 26–33 km indicate hypocentres of earthquakes of magnitude >6 in the Hazara Kashmir syntaxis since 1974, projected horizontally on the profile AA' (Figure 2). They approximately coincide with the lower interface of the upper and intermediate layers.

which generally provides the approximate depths to the sources located along a particular layer¹⁵. In the present case, the computed spectrum (see Figure 5) can be approximated by five linear segments with slopes equivalent to 127, 61, 37, 27 and 13 km, which appear to represent approximately average depths to base of the lithosphere, Moho (61 km), mid-crustal interfaces (37, 27 km) and the upper crust (13 km) respectively, in this region. The mid-crustal interfaces may represent an intermediate zone separating the upper and lower crusts.

We selected a gravity profile AA' (Figure 2) extending from south of Lahore–Sargodha ridge (H1) to Tarim basin (H3) across the epicentral zone of this earthquake and other important tectonic elements of this region. This profile is chosen so as to be almost perpendicular to the major gravity/structural trends in the region. This profile (Figure 4) also shows almost flat topography on either sides representing foredeeps on two sides, which can be used as constraints for crustal thickness in the model. As discussed above, Figure 4 shows a gravity high (H1) for the Lahore–Sargodha ridge, which is related to the flexural bulge and a large wavelength and large amplitude gravity low (L1) over the Karakoram range towards the north, related to crustal thickening caused by the Himalayan orogeny. Superimposed over this large wavelength gravity low (L1), there are small wavelength and amplitude gravity high and low (H2 and L2) related to Altn Tagh Fault (ATF) and Tarim basin respectively. With the average depth of important subsurface interfaces obtained from

spectral decay (Figure 5), the profile AA' is modelled as given at the bottom of Figure 4. The lithosphere–asthenosphere boundary (LAB) is constrained based on *S*-wave receiver function analysis in the northern and southern parts of the profile as 100 km dipping in the central part¹⁶ up to 160 km, whose average depth matches well with those obtained from spectral analysis (127 km; Figure 5). The LAB based on receiver function analysis¹⁶, shows sudden depth of 250–260 km of Eurasian plate under Karakoram which however, is not included in the gravity model due to limitations in the gravity data resolution. However, the effect of LAB on computed field would be small due to large depth and small density contrast. Some constraints to model subsurface structures along this profile are also obtained from the results of deep seismic profiles^{11,12} and gravity crustal models¹⁰. The computed crustal model shows variation in crustal thickness from about 40 km in the foredeep towards south, deepening to almost 70 km under the Karakoram range, which almost rises to about 45 km under the Tarim basin. It is interesting to note that towards north over Tarim basin the topography is about 1000 m (flat), while towards south of Lahore–Sargodha ridge, it is about 200 m (flat). Accordingly the crustal thickness is about 5 km thicker towards north compared to south according to isostatic balance. This model also shows a low density body at the surface under the Karakoram range representing a granitic batholith. The small gravity high and low (H2 and L2) are modelled due to intrusive of high density rocks and sediments of the Tarim basin. The Lahore–Sargodha high (H1) is modelled due to flexural bulge, which shows an uplift of both Moho and the basement.

An intermediate layer between 15 and 30 km separates the upper and lower crusts. Crustal thickness under the Karakoram–Hindukush range is largest and so is its elevation at the surface. This indicates that Hindukush–

Karakoram form the central core complex of collision tectonics, with opposite dipping thrusts on either side. The uplift of Moho under Lahore–Sargodha ridge is part of the lithospheric flexure and can generally be attributed to the load of the Himalayas, which will cause compression at the lower interface of the crust, while at the upper part it will experience an extensional force in the opposite direction (Figure 4). The flexural bulge in the Himalayan Foredeep is most prominent in this section in the form of the Lahore–Sargodha ridge compared to those towards the east (H1–H3; Figure 3), where it could be delineated only after low-pass-filtering of the original map⁷. The prominent flexural bulge of the Lahore–Sargodha ridge will contribute to stress build-up in this section (Figure 4). It may be noted here that the hypocentre of seismic activity in this section mostly lies² at depths of about 10–15 and 25–35 km, which approximately coincides with the lower boundaries of the upper crust and intermediate layer (Figure 4). For example, since 1974, six earthquakes of magnitude >6, two each of focal depths 10, 26 and 33 km, have been reported from Hazara Kashmir syntaxis, which almost coincide with the lower boundary of the upper crust and intermediate layer, when projected on profile AA' (Figure 4). Some departures of these hypocentres from these interfaces can be attributed to ambiguity in modelling gravity field and profile AA' is located east of this syntaxis. In fact, these interfaces may not be represented by sharp boundaries but instead by diffused zones of a few kilometres in width. These observations indicate that these two interfaces are primarily seismogenic in this region. The lower interface of the intermediate layer (30–32 km) may also represent the interface separating the upper brittle and lower ductile crusts as effective elastic thickness under the western part of the Himalayas and foredeep^{17,18} varies between 25 and 35 km. Almost at same depth of about 25–30 km, a conductive layer based

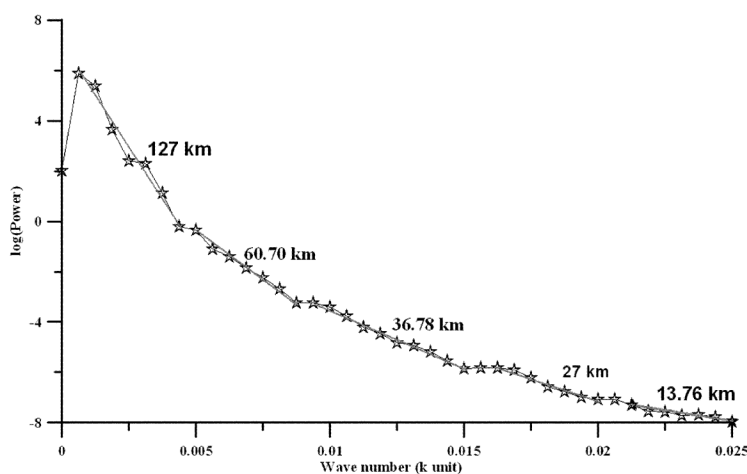


Figure 5. Spectrum of Bouguer anomaly map of NW Himalayas (Figure 2), showing five linear segments with slopes proportional to 127.0, 60.7, 36.8, 27.0 and 13.0 km, which provide average depths to the interfaces represented by them¹⁵.

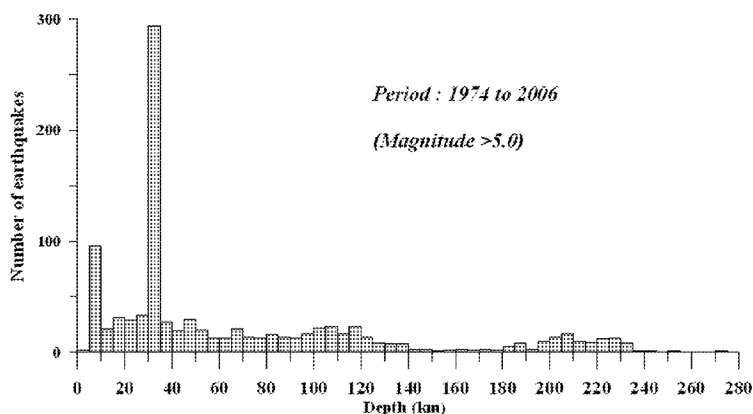


Figure 6. Histogram of earthquakes of magnitude² greater than 5 since 1974 showing their concentration in depth range of 5–10 and 30–35 km, which generally coincides with basement and lower boundary of intermediate layer.

on magnetotelluric results¹⁹ has been suggested along southern Tibet and west of it, which also indicates that below this level the crust may be ductile in nature. It is also indicated by low velocity²⁰ and low density⁸ layer almost at the same depth in this section. It may be extending even in the western Himalayas west of Tibet, as indicated by low velocity¹¹ and low density¹⁰ layer in this region. The histogram of the number earthquakes of magnitude greater than five along the southern Himalayan front and focal depth (Figure 6) also suggest their concentration in the depth range of 5–10 and 30–35 km. In this regard it may be added here that some of the shallow-focus earthquakes (~10 km) show normal faulting while those originating from deeper levels (> 25 km) indicate thrust faulting²¹ as in the case of the Kashmir earthquake of 8 October 2005. This indicates the importance of extensional tectonics at the basement level and compressional forces at deeper levels due to flexural bulge. Some correlation between effective elastic thickness and depth to seismogenic layer has been found in most of the active convergent zones in the world^{22,23}.

The load of the Himalayas on the Indian plate is analogous to a cantilever beam; more the sediments in the foredeep, more stable will it be. Therefore lack of sediments in the foredeep and over the basement flexural bulge in this section²⁴, makes this region comparatively more unstable compared to other parts of the Himalayas, which is also indicated by faster uplift of Nanga Parbat²⁵ NE of the epicentre of this earthquake compared to other parts. A large positive shear vertical stress is required to produce the observed topography in this section¹³, which would produce large bending moment at the end of the Indian plate causing a prominent flexural bulge, as is presently observed in this region. Flexural rigidity of the Indian crust in this part is estimated¹³ as $4.0 [\pm 2.0] \times 10^{23}$ Nm, which is a factor of ten less than the Central and Eastern Himalayas indicating a weak crust.

Present-day seismic activity in the southern Himalayan front is concentrated south of the MCT and is attributed

to decollement of the Indian crust along the Himalayan frontal thrust²⁶. In fact, decollement of the Indian crust might have been caused by extensional forces in the upper crust due to flexural bulge as shown in Figure 4, which will add to the plate tectonic forces at the shallow level, while at deeper levels in the lower crust it is opposite to the plate tectonic forces. At an intermediate level there will be a neutral plane²¹ where these two forces, viz. extensional at the top and compressional in the lower crust will cancel each other. This would produce differential stress in the crust, resulting into decoupling of the upper and lower parts of the Indian crust and a weak intermediate crust. Flexural bulge in the present case is analogous to forebulges in the case of oceanic trenches, which cause considerable stress in the part of the bulge towards the trench²⁷. High conductivity¹⁹ and low velocity²⁰ along the southern part of Tibet and north of it²⁸ under Tien Shan (Asian plate) at mid crustal level, suggest the presence of large amount of fluids in this region which might have been caused by subduction, collision and magmatism in the region. In case weak intermediate crust filled with fluids is caused by specific orogeny of this region, it should be present in the entire region, including Tibet and southern part of Eurasian plate²⁸ as indicated above. In such a case, almost flat topography of Tibet and its uplift as plateau might have been partly caused by the presence of fluids at intermediate crustal level in the entire region due to its buoyancy. The role of fluids for triggering of earthquakes has been highlighted in several cases, specially in fore-arc regions²⁹.

It may be further noted that the southern side of gravity highs (H1–H3) representing flexural bulge along the Himalayan foredeep and H4 in the western part, coincides with Narmada–Son lineament (Jabalpur earthquake, 1997, H2), Shillong Plateau (H3) and Kutch (H4) respectively (Figure 3), which are also relatively active zones³⁰, indicating the importance of flexural bulge for near-plate boundary seismic activity. In the present case (Figure 3) the epicentre of the Jabalpur earthquake coincides with

the southern flank of the flexural bulge, that would experience maximum stress instead of top of it, as suggested previously³¹. It is interesting to note that the focal depth of the Jabalpur earthquake is reported as 35 km and the effective elastic thickness (EET)³² in the southern part of the Himalayan foredeep is also 35 km, thereby indicating that even for intra plate seismicity, transition from brittle to ductile part of the crust plays an important role as in case of plate boundary earthquakes as described above. This also indicates that while in collision zones, the lithospheric strength resides in the upper crust, in case of cratons the whole crust or even the uppermost mantle where EET is large exhibits strength. Therefore, a single model cannot be generalized for strength of the lithosphere in all regions as suggested previously³³ which is also indicated by large variations in EET in different geological provinces. In fact it will largely depend on tectonic history, thermal history, composition and crustal structure in a region.

1. Rajendran, C. P. and Rajendran, K., The status of central seismic gap: a perspective based on the spatial and temporal aspects of the large Himalayan earthquakes. *Tectonophysics*, 2005, **395**, 19–39.
2. http://neic.usgs.gov/neis/epic/epic_rect.html
3. Seeber, L., Armbruster, J. G. and Quittmeyer, R. C., Seismicity and continental subduction in the Himalayan arc. In *Zagros, Hindu Kush, Himalaya; Geodynamic Evolution*, Geodynamics Series, 1981, vol. 3, pp. 215–242.
4. Marussi, A. and Ebbin, The tectonic scheme of central Asia (compiled), Bouguer anomaly map (1975). *Ace. Naz. Lincei*, 1976, **21**, 131–137.
5. Caporali, A., The gravity field of the Karakoram mountain range and surrounding areas. *Geol. Soc. London, Spl. Publ.*, 2000, **170**, 7–23.
6. *Bouguer Anomaly Map of Western ESCAP Region*, UNESCO Publication, 1976.
7. Mishra, D. C., Laxman, G. and Arora, K., Large-wavelength gravity anomalies over the Indian continent: Indicators of lithospheric flexure and uplift and subsidence of Indian Peninsular Shield related to isostasy. *Curr. Sci.*, 2004, **86**, 861–867.
8. Rajesh, R. S. and Mishra, D. C., Admittance analysis and modeling of satellite gravity over Himalayas–Tibet and its seismogenic correlation. *Curr. Sci.*, 2003, **84**, 224–230.
9. Bilham, R., Gaur, V. K. and Molnar, P., Himalayan seismic hazard. *Science*, 2001, **293**, 1442–1444.
10. Mishra, D. C., Crustal structure and dynamics under Himalaya and Pamir ranges. *Earth Planet. Sci. Lett.*, 1982, **57**, 415–420.
11. Finetti, I., Giorgetti, F. and Poretti, G., The Pakistani segment of the DSS-profile Nanga Parbat–Karakul (1974–1975). *Boll. Geofis. Tear. Appl.*, 1979, **21**, 159–171.
12. Kaila, K. L., Krishna, V. G., Roychowdhury, K. and Hari Narain, Structure of the Kashmir Himalaya from deep seismic soundings. *J. Geol. Soc. India*, 1978, **19**, 1–20.
13. Duroy, Y., Farah, A. and Lillie, R. J., Subsurface densities and lithospheric flexure of the Himalayan foreland in Pakistan. In *Tectonics of the Western Himalayas*, Geol. Soc. America, Spl. Pap., 1989, 232, pp. 217–236.
14. Malinconico Jr., L. L., Crustal thickness estimates for the western Himalaya, In *Tectonics of the Western Himalayas*, Geol. Soc. America, Spl. Pap., 1989, 232, pp. 237–242.
15. Mishra, D. C. and Pedersen, L. B., Statistical analysis of potential fields from subsurface reliefs. *Geoexploration*, 1982, **19**, 247–265.
16. Kumar, P., Yuan, X., Kind, R. and Kosarev, G., The lithosphere–asthenosphere boundary in the Tien Shan–Karakoram region from S-receiver functions: Evidence for continental subduction. *Geophys. Res. Lett.*, 2005, **32**, L07305.
17. Rajesh, R. S. and Mishra, D. C., Lithospheric thickness and mechanical strength of the Indian shield. *Earth Planet. Sci. Lett.*, 2004, **225**, 319–328.
18. Jordan, T. A. and Watts, A. B., Gravity anomalies, flexure and the elastic thickness structure of the India–Eurasia collisional system. *Earth Planet. Sci. Lett.*, 2005, **236**, 732–750.
19. Unsworth, M. J., Jones, A. G., Wei, W., Marquis, G., Gokarn, S. G., Spratl, J. E. and INDEPTH M. T. Team, Crustal rheology of the Himalaya and southern Tibet inferred from magnetotelluric data. *Nature*, 2005, **438**, 79–81.
20. Zhao, Z. and Nelson, K. D., Project INDEPTH Team, Deep seismic reflection evidence for continental underthrusting beneath southern Tibet. *Nature*, 1993, **361**, 557–559.
21. Jackson, J., Strength of the continental lithosphere: Time to abandon the jelly sandwich? *GSA Today*, 2002, **12**, 4–9.
22. Chen, W. P. and Molnar, P., Focal depths of intra continental earthquakes and their implications for thermal and mechanical properties of the lithosphere. *J. Geophys. Res.*, 1983, **88**, 4183–4214.
23. Watts, A. B., *Isostasy and Flexure of Lithosphere*, Cambridge University Press, Cambridge, 2001, pp. 281–284.
24. *Seismotectonic Atlas of India and its Environs*, Geol. Surv. India Publ., 2000.
25. Whittington, A. G., Exhumation overrated at Nanga Parbat, northern Pakistan. *Tectonophysics*, 1996, **260**, 215–226.
26. Ni, J. and Barazangi, M., Seismotectonics of the Himalayan collision zone; geometry of the underthrusting Indian Plate beneath the Himalaya. *J. Geophys. Res.*, 1984, **89**, 1147–1163.
27. Turcotte, D. L. and Schubert, G., *Geodynamics*, Cambridge University Press, Cambridge, 2002, pp. 1–441.
28. Vinnik, L. P., Roecker, S., Kosarev, G. L., Oreshin, S. I. and Koulikov, I. Y., Crustal structure and dynamics of the Tien Shan. *Geophys. Res. Lett.*, 2002, **29**, 2047.
29. Mishra, O. P., Zhao, D., Umino, N. and Hasegawa, A., Tomography of northeast Japan forearc and its implications for interplate seismic coupling. *Geophys. Res. Lett.*, 2003, **30**, 1850.
30. Mishra, D. C. and Rajsekhar, R. P., Bhuj earthquake of 26 January 2001 and comparison with Shillong earthquake of 1897: Tectonic inversion, Lithospheric flexure and plate motion. *Curr. Sci.*, 2006 (in press).
31. Bilham, R., Bendick, R. and Wallace, K., Flexure of the Indian Plate and intraplate earthquakes. *Proc. Indian Acad. Sci.*, 2003, **112**, 315–329.
32. Rajesh, R. S., Stephen, J. and Mishra, D. C., Isostatic response and anisotropy of eastern Himalayan–Tibetan Plateau: a reappraisal using multi taper spectral analysis. *Geophys. Res. Lett.*, 2003, **30**, 32–1–4.
33. Burov, E. B. and Watts, A. B., The long term strength of continental lithosphere: ‘jelly sandwich’ or ‘crème brulee’. *GSA Today*, 2006, **16**, 4–10.
34. Hanson, C. R., The northern suture in the Shigar Valley, Baltistan, northern Pakistan. *Geol. Soc. Am., Spec. Pap.*, 1989, **232**, 203–215.

ACKNOWLEDGEMENTS. We thank the Director, NGRI, Hyderabad and CSIR, New Delhi for permission to publish this work and the Emeritus Scientist Scheme. Suggestions by an anonymous reviewer helped improve an earlier version of the manuscript. Thanks are also due to Dr V. M. Tiwari for suggestions and Mr Ch. Ramaswamy for preparation of the manuscript.

Received 21 November 2005; revised accepted 21 January 2006